12C.4 VORTEX HEIGHT EVOLUTION DURING TROPICAL CYCLONE RAPID INTENSIFICATION

Alexander J. DesRosiers[1] and Michael M. Bell[1]
[1]Colorado State University, Fort Collins, CO

1. INTRODUCTION

Predicting the rapid intensification (RI) of tropical cyclones (TCs) requires understanding of internal intensity change mechanisms in addition to environmental predictors (Hendricks et al., 2010). Recent research efforts have improved our understanding of the role TC radial and azimuthal wind structure plays in RI, but much still remains to be learned about TC vertical structure (Chen et al., 2023). In DesRosiers et al. (2023), henceforth D23, relationships between the height of the TC vortex, intensity, and intensity change were characterized in the Tropical Cyclone Radar Archive of Doppler Analyses with Recentering dataset (TC-RADAR; Fischer et al., 2022) which is composed of kinematic analyses of TCs observed by aircraft with tail Doppler radar (TDR).

D23 introduced the dynamic height of the TC vortex (DHOV) metric which is defined as the height at which the maximum winds in the azimuthally-averaged tangential wind field decay to 40% of the maximum at 2-km altitude in each analysis. The reduced dependence on the current TC intensity through the normalization allowed for evaluation of TC vertical structure relationship to intensity change. Larger DHOV values were found to favor TC intensification, with a deep vertical vortex structure present in all observed cases which met a pressure-based RI definition in the 24-hour period following the observations. D23 also found a strong relationship between DHOV and vertical wind shear (VWS), which acts to tilt the vortex downshear. The tilt causes the low- and mid-level circulation to become vertically misaligned, which inhibits intensification (Demaria, 1996). However, once the vortex becomes aligned, vertical growth of the vortex can continue. This vertical growth was observed and characterized in TDR observations during the RI of Hurricane Michael (2018) as both a dynamic and kinematic process in the upper levels of the atmosphere (DesRosiers et al., 2022). The DHOV metric contains information about VWS-induced tilt, vertical vortex development, and the TC warm core, and therefore holds promise as a diagnostic value that encapsulates the effects of multiple processes throughout the TC lifecycle and possible predictor for RI. In this study, we further investigate the DHOV metric and its relationship to TC structural changes occurring during RI.

2. DATA AND METHODS

The TC-RADAR dataset is revisited to clarify the role of vortex tilt in determining DHOV in observed storms. Vortex tilt values are calculated between 1- and 6-km altitude to compare the distribution of DHOV values between observed TCs with and without vortex tilt. Since the TC-RADAR dataset contains snapshots, a 20-member WRF ensemble simulation of idealized TCs used in Tao and Zhang (2014) and Nam et al (2023) is used to investigate the evolution of DHOV in moderate deep-layer VWS. Each of the ensemble simulations is initialized with a modified Rankine vortex profile with a 15 m s^{-1} tangential wind maximum at 135-km radius. VWS with a moderate magnitude of 7.5 m s^{-1} is imposed in an otherwise favorable thermodynamic environment for TCs. Several kinematic and thermodynamic quantities are tracked in each ensemble member as the simulated TCs align and undergo RI.

A pair of additional idealized modeling simulations are performed using Cloud Model 1 (CM1) to focus on the importance of upper-level development to DHOV and TC intensification. In contrast to the WRF ensemble, the CM1 simulations include parameterized radiation and concentrate the VWS layer in the upper troposphere. A control (CTRL) simulation has no background flow while a parallel simulation evolves in the presence of a 7.5 m s^{-1} upper-level zonal jet (ULJET). DHOV and additional metrics are calculated to understand the sensitivity of DHOV and intensity to changes in TC vertical structure in the upper levels of the troposphere.

3. RESULTS

3.1 OBSERVATIONAL ANALYSIS

As in D23, intensity change groups are determined by the 24-hour rate of change in minimum sea level pressure (P_{min}) following analysis time. RI is defined as a drop in P_{min} greater than 21 hPa, strengthening storms that do not meet the RI threshold are in the intensifying group (IN), and changes in pressure from -5 to +5 hPa classify as steady-state (SS). The distribution of DHOV values narrows towards exclusively high values (DHOV ≥ 10 km) in the RI group (Fig. 1a). When reducing the sample to only aligned vortices (defined as tilt magnitude < 10 km), all observed cases exhibit DHOV of 10 km or greater (Fig. 1b), consistent with the RI group. Tilted vortices do not project strong tangential winds in the azimuthal mean that is used to determine DHOV. It is important to note from Fig. 1 that there are no observed instances of “short” TCs in the aligned group, indicating the TCs with DHOV metric less than 10 km were just vertically misaligned, rather than being shallow, aligned vortices.

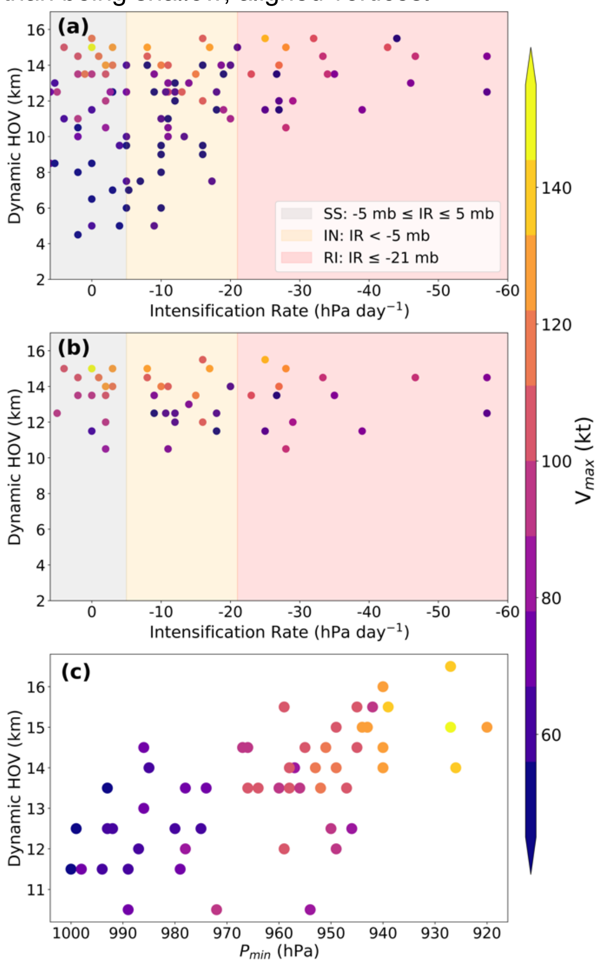

FIG. 1. (a) DHOV as a function of intensity change with shading representing steady-state (SS), intensifying (IN), and rapidly intensifying (RI) groups with intensification rate (IR) bounds defined (legend). (b) Cases from (a) with vortex tilt < 10 km magnitude. (c) DHOV as a function of intensity (Pressure; hPa) in aligned cases colored by maximum sustained winds (V_{max}).

When DHOV is plotted with respect to intensity in the aligned cases there is an increasing trend (Fig. 1c), such that stronger aligned storms tend to have higher DHOV. The trend is weakest in weaker storms with considerable spread of DHOV values, but as TCs approach and attain major hurricane intensity (Category 3+; P_{min} ≤ 960 hPa), the upward trend indicates continued vertical growth and intensification of the tangential wind field. The observational analysis indicates that DHOV contains useful information about vertical structure in both tilted and aligned TCs, with values less than 10 km indicating tilted storms, and values above 10 km in aligned storms scaling with intensity.

3.2 NUMERICAL MODEL ANALYSIS

The simulated TCs in all members of the WRF ensemble experience initial vortex tilt, followed by alignment, RI, and steady-state extreme intensity (Category 4+) with varied timing (not shown). When the evolution is adjusted to a common alignment time (Fig. 2), the evolution of each member is similar. As the low- and mid-level centers come into alignment, there is an upward jump in DHOV values (Fig. 2b). The jump in DHOV is denoted as the time of “adequate” alignment where the alignment process has not yet completed, but which precedes RI onset. When all members are temporally centered on this time, three distinct phases of intensification emerge.

The phase prior to the DHOV jump is termed the pre-alignment phase (green shading; Fig. 2) and characterized by slow intensification, small DHOV, and large vortex tilt. The active alignment phase (yellow shading; Fig. 2) is a 36-hour period which begins with reduction of tilt and ends with RI onset. During active alignment, a steep increase in DHOV occurs followed by a brief reduction in the metric as an upper-level warm core forms (not shown). The post-alignment vertical growth phase (red shading; Fig. 2) is characterized by rapidly falling P_{min}, and rising DHOV as vertical growth of the vortex and RI continue in the absence of vortex tilt. The three regimes of intensification identified in the WRF ensemble analysis appear in a consistent fashion in all members when time is centered on the jump in DHOV. The consistent evolution across members indicates the importance of vortex tilt to DHOV as well as the continued relevance of this metric throughout the RI process.

In the CM1 simulations (not shown), the increasing vertical extent of the vortex in concert with development and intensification of the upper-level component of the TC warm core is further investigated and are briefly summarized here. Differences in the duration of RI and the peak steady-state intensities reached in the two idealized TCs simulated in CM1 are related to intensification in the post-alignment vertical growth phase. In the ULJET simulation, RI onset and intensification initially proceed similarly to the CTRL simulation since the VWS is restricted to the upper troposphere. However, as the vortex grows upward toward the influence of the upper-level jet, the vertical development of the vortex and warm core are halted. Intensification ceases as well, and the storm never reaches the extreme intensity of CTRL. The effective capping of DHOV and intensity in ULJET suggests vertical growth of the vortex may be a key factor in a storm's ability to achieve extreme intensity. Structural changes in the upper levels of the simulated TC vortices in both CM1 experiments will be discussed in detail at the conference.

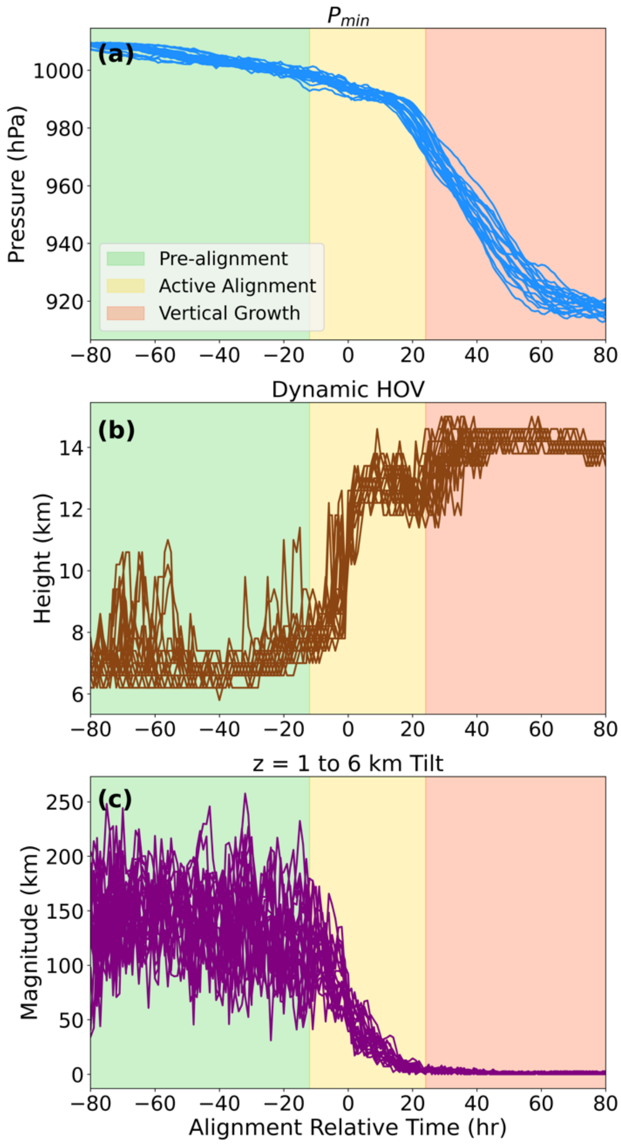

FIG. 2. Time series for WRF ensemble members of (a) Pmin, (b) DHOV, and (c) 1 to 6 km vortex tilt magnitude. Stages denoted by colors of the background shading (legend; a).

4. CONCLUSIONS

The DHOV metric for vortex height is shown to be a useful diagnostic for structure and intensity change in TCs. The metric can be viewed as having information about three phases of intensification: pre-alignment, active alignment, and post-alignment vertical growth. Numerical model simulations and observations indicate that VWS-induced vortex tilt decreases DHOV by reducing the strength of the azimuthally-averaged tangential wind field at higher altitudes during the pre-alignment phase. During active vortex alignment, there is a jump in DHOV above 10 km that precedes RI. Once alignment is complete and an upper-level warm core forms, DHOV continues to increase via intensification of the upper-level tangential wind field and TC warm core via the mechanisms described in DesRosiers et al. (2022). CM1 simulations indicate that upper-level VWS can cap the post-alignment vertical growth phase which can limit the peak intensity a TC may attain. The interpretation of DHOV obtained from radar observations and idealized modeling experiments improves our understanding of the role TC vertical structure plays in the RI process, and suggests that DHOV is a useful diagnostic for intensity prediction.

Acknowledgements This research is supported by ONR Award N000142012069 under the Tropical Cyclone Rapid Intensification DRI.

REFERENCES

Chen, X., and Coauthors, 2023:Research Advances on Internal Processes Affecting Tropical Cyclone Intensity Change from 2018-2022. *Tropical Cyclone Res. and Rev.*, **12**, 10–29, doi: https://doi.org/10.1016/j.tcrr.2023.05.001.

DeMaria, M., 1996: The Effect of Vertical Shear on Tropical Cyclone Intensity Change. *Jour. Of the Atmos. Sci.*, **53**, doi: https://doi.org/10.1175/1520-0469(1996)053<2076:TEOVSO>2.0.CO;2.

DesRosiers, A. J., Bell, M. M., and Cha, T. Y., 2022: Vertical Vortex Development in Hurricane Michael (2018) during Rapid Intensification. *Mon. Wea. Rev.*, **150**, 99–114, doi: 10.1175/MWR-D-21-0098.1.

DesRosiers, A. J., and Coauthors, 2023: Observed Relationships between Tropical Cyclone Vortex Height, Intensity, and Intensification Rate. *Geo. Res. Lett.*, **50**, e2022GL101877, doi: https://doi.org/10.1029/2022GL101877.

Fischer, M. S., and Coauthors, 2022: An Analysis of Tropical Cyclone Vortex and Convective Characteristics in Relation to Storm Intensity Using a Novel Airborne Doppler Radar Database. *Mon. Wea. Rev.*, **150**, 2255-2278, doi: https://doi.org/10.1175/MWR-D-21-0223.1.

Hendricks, E. A., and Coauthors, 2010: Quantifying Environmental Control on Tropical Cyclone Intensity Change. *Mon. Wea. Rev.*, **138**, 3243–3271, doi: https://doi.org/10.1175/2010MWR3185.1.

Nam, C. C., M. M. Bell, and D. Tao, 2023: Bifurcation points for tropical cyclone genesis in sheared and dry environments. *J. Atmos. Sci,* **80**, 2239–2259. doi: https://doi.org/10.1175/JAS-D-22-0100.1 .

Tao, D. and F. Zhang, 2014: Effect of environmental shear, sea-surface temperature, and ambient moisture on the formation and predictability of tropical cyclones: An ensemble-mean perspective. *J. Adv. Model. Earth Syst.*, **6**, 384–404, doi: https://doi.org/10.1002/2014MS000314.